Chapter

Characteristics of Atrial Premature Beat ECG Signals on Variant Maps

Lihua Leng, Jeffery Zheng and Jing Zhang

Abstract

Premature heartbeat is also known as extrasystole. It means the foundation of sinus or ectopic heart rhythm, a certain pacemaker in the heart excitable earlier than the basic rhythm, cause the heart to be local or all happening prematurely remove pole. Premature atrial beats may lead to cardiomyopathy. The experimental data in this chapter are provided by Xishan People's Hospital of Wuxi city, including normal ECG signals and abnormal ECG signals (atrial premature beat). The two types of ECG data sequences are processed experimentally through the variant measurement model, and the differences in the variant maps are compared.

Keywords: atrial premature beat, ECG signal, data sequence, arrhythmia, variant maps

1. Introduction

Cardiovascular diseases are common diseases that seriously threaten human health [1], and the mortality rate caused by cardiovascular diseases continues to increase globally. ECG signal is the direct response of heart activity and the most effective way to analyze cardiovascular diseases. The object of this chapter is the atrial premature beat ECG signal in atrial arrhythmia. The experimental method is variant measurement model [2]. The provider of ECG data is Xishan People's Hospital of Wuxi city, Jiangsu Province China, and the later calibrator of ECG data is the First People's Hospital of Yunnan Province China. This chapter includes relevant background to introduce atrial premature beat [3], variant measurement model, experimental data, and variant maps of atrial premature beat signals. There is a significant difference between the variant maps of normal and atrial premature beat ECG signals obtained through variant measurement schemes.

This chapter uses the variant measurement model and the visualization method of feature clustering to study the variant measurement of ECG signal data sequences. ECG signal utilizes multivalued logic function and variant principle to form variant logic symbol on n-element ECG signal sequence and output variant maps and observe the difference between different ECG signal data. The obtained variant maps can analyze the ECG data from the macroscopic level and express the information that cannot be reflected by the traditional ECG in an intuitive way. The application of variant maps in ECG signal is an extension of the original ECG signal methods. In practical applications, it is expected that the variant maps can assist the application of traditional ECG in the medical field and help clinicians to diagnose the test results more conveniently.

2. Relevant background

2.1 Atrial premature beats

Atrial arrhythmia is the most common arrhythmia clinically, which refers to a kind of arrhythmia caused by conduction obstruction when ectopic excitations are located in the atrium or conduction system passing through the atrium. It is mainly active arrhythmia, and atrial premature beat is the most common type of atrial arrhythmia. Atrial premature beats can be seen in normal healthy people, but in healthy people, there are few frequent atrial premature beats [4]. Atrial premature beats is more common in organic heart disease patients, Hyperthyroidism, Coronary heart disease, Cardiomyopathy patients if frequent atrial premature beat, is the precursor of Atrial fibrillation, Acute myocardial infarction can also occur frequent atrial premature beat. **Figure 1** shows the comparison between normal ECG and atrial premature beat ECG.

The picture is the atrial premature beat ECG. Patient information: male, 46 years old, arrhythmia, mean heart rate 62 bpm, early occurrence of P′-QRS-T in limb leads, 160 ms in P'R interval, incomplete compensatory interval, such expression is a atrial premature beat.

2.2 Variant measurement model

In 2010, variant model [5] was proposed with the stability of cellular automata as an example; the effect of variant and non-variant functions on binary logic functional space was explained. In 2011, the conditional probability statistical distribution of the variant measurement structure [6] is discussed. By simulating the two-state quantum interaction system, the variant two-path simulation model was established. With the continuous development of variant construction, this model has been applied in many fields: coding and non-coding DNA [7] sequence detection, random sequence testing [8], classification of cellular automata [7], classification of echolocation in bats [9], ECG signals [10, 11], and variant construction [12].

2.3 Variant logic

The core theory of variant measurement model is variant logic, which is extended and evolved on the basis of classical logic. In the variant logic function, assuming that the input sequence is N long $\{X, 0 \le i < N\}$, the output data sequence $\{Y, 0 \le i < N\}$ is N-1 according to the variant rule. On the basis of the variant logical function, the variant measurement model defines four basic variant logical symbols:

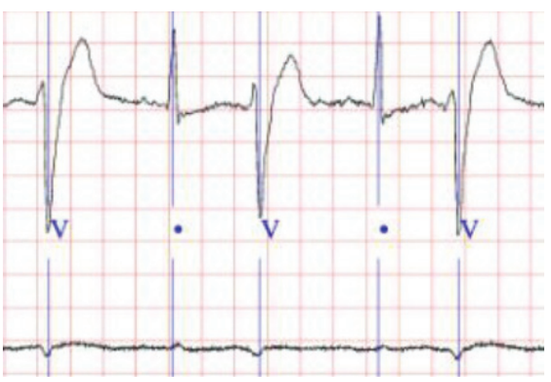

Figure 1.
Atrial premature beats ECG.

$\{+, -, \top, \perp\}$. The transformation rules of the four variant symbols are shown in **Table 1**. Therefore, in this chapter, N long ECG signal is converted into $N-1$ long variant logical operator through variant logical function.

2.4 Variant visualization

The variant measurement model describes the measurement as the four meta symbols: $\{+, -, \top, \perp\}$. The 16 subsets of meta symbol set are as follows: $\{\emptyset\}$, $\{+\}$, $\{-\}$, $\{\top\}$, $\{\perp\}$, $\{+, -\}$, $\{+, \perp\}$, $\{+, \top\}$, $\{-, \top\}$, $\{-, \perp\}$, $\{\perp, \top\}$, $\{+, -, \top\}$, $\{+, -, \perp\}$, $\{+, \top, \perp\}$, $\{-, \top, \perp\}$, and $\{+, -, \top, \perp\}$.

The 16 subsets correspond to the 16 measures: $M_0, M_1, M_2, M_3, M_4, M_5, M_6, M_7, M_8, M_9, M_{10}, M_{11}, M_{12}, M_{13}, M_{14}, M_{15}$. Here, the statistical quantity of $\{\emptyset\}$ is defined as 0 and the corresponding definitions of 16 variant measures are shown in **Table 2**.

If any measure is selected as the value of χ in the variant maps and any measure is selected as the value of γ in the variant maps, there are a total of $16 * 16 = 256$ combinations of such two-dimensional maps, which are specifically shown in **Table 3**. In this chapter, the three-dimensional variant maps are also adopted, and the Z-axis is added on the basis of the two-dimensional maps. The selection principle is the same as the selection method of χ and γ.

2.5 ECG signal variant measurement structure

Variant measurement structure is composed of three components: input, processing, and output. The input ECG signal is provided by Wuxi Xishan People's Hospital. The data processing module is the core module of variant measurement and consists of variant module, statistical measurement module, and visualization

Conversion type	Variant sign	Statistical sign	Statistical total
$0 \to 0$	$\perp$	$N_\perp$	$N = N_\perp + N_+ + N_- + N_\top$
$0 \to 1$	$+$	N_+	
$1 \to 0$	$-$	N_-	
$1 \to 1$	$\top$	$N_\top$	

Table 1.
Variant sign conversion rule.

Sign subset	Variant measure	Sign subset	Variant measure
$\{\emptyset\}$	$M_0 = 0$	$\{-, \top\}$	$M_8 = N_- + N_\top$
$\{+\}$	$M_1 = N_+$	$\{-, \perp\}$	$M_9 = N_- + N_\perp$
$\{-\}$	$M_2 = N_-$	$\{\perp, \top\}$	$M_{10} = N_\perp + N_\top$
$\{\top\}$	$M_3 = N_\top$	$\{+, -, \top\}$	$M_{11} = N_+ + N_- + N_\top$
$\{\perp\}$	$M_4 = N_\perp$	$\{+, -, \perp\}$	$M_{12} = N_+ + N_- + N_\perp$
$\{+, -\}$	$M_5 = N_+ + N_-$	$\{+, \top, \perp\}$	$M_{13} = N_+ + N_\top + N_\perp$
$\{+, \perp\}$	$M_6 = N_+ + N_\perp$	$\{-, \top, \perp\}$	$M_{14} = N_- + N_\top + N_\perp$
$\{+, \top\}$	$M_7 = N_+ + N_\top$	$\{+, -, \top, \perp\}$	$M_{15} = N_+ + N_- + N_\top + N_\perp$

Table 2.
Definition of 16 variant measures.

X / Y	M_0	M_1	...	M	M_{15}
M_{15}	(M_0, M_{15})	(M_1, M_{15})	...	(M_{14}, M_{15})	(M_{15}, M_{15})
M_{14}	(M_0, M_{14})	(M_1, M_{14})	...	(M_{14}, M_{14})	(M_{15}, M_{14})
...	...	...	...	...	...
M_1	(M_0, M_1)	(M_1, M_1)	...	(M_{14}, M_1)	(M_{15}, M_1)
M_0	(M_0, M_0)	(M_1, M_0)	...	(M_{14}, M_0)	(M_{15}, M_0)

Table 3.
Combinations of visualization of 256 variant measures.

Figure 2.
Structure diagram of ECG sequence variant measurement.

module. The final output is variant maps. The structure of ECG signal variant measurement is shown in **Figure 2**.

2.6 Data processing module

The data processing module is divided into three parts: variant module, measurement statistics module, and visualization module. The variant module is the most important part of the variant measurement model. It is mainly responsible for transforming the original ECG signal sequence into the sequence of four basic variant logic symbols $\{+, -, \top, \perp\}$ through mapping rules. The specific definitions of the parameters X, T, L, V involved in the transformation process will be given in the core module. The measurement statistics module is mainly responsible for grouping the variant logical symbol $\{+, -, \top, \perp\}$ sequence by setting a reasonable segment length M according to total length of the sequence. After grouping, the $\{+, -, \top, \perp\}$ sequence in each group is counted and denoted as $\{N_+, N_-, N_\top, N_\perp\}$. The visualization module is to generate the final variant maps, in which the variant maps can be two-dimensional map and three-dimensional map. The specific visualization process will be given in the chapter of the core module. The structure diagram of the data processing module is shown in **Figure 3**.

2.7 Core module

2.7.1 Variant module

The variant module is the most core module in the variant measurement model. It is mainly responsible for converting the obtained ECG signal sequence into four variant logical symbol $\{+, -, \top, \perp\}$ sequences through variant logic. The transformation process involves parameters X, T, L, V, and the definition is shown in Eqs. (1)–(4).

$$X = A_{i+1} - A_i \tag{1}$$

$$T = \frac{\sum_{i=1}^{N-1} |A_{i+1} - A_i|}{N} \tag{2}$$

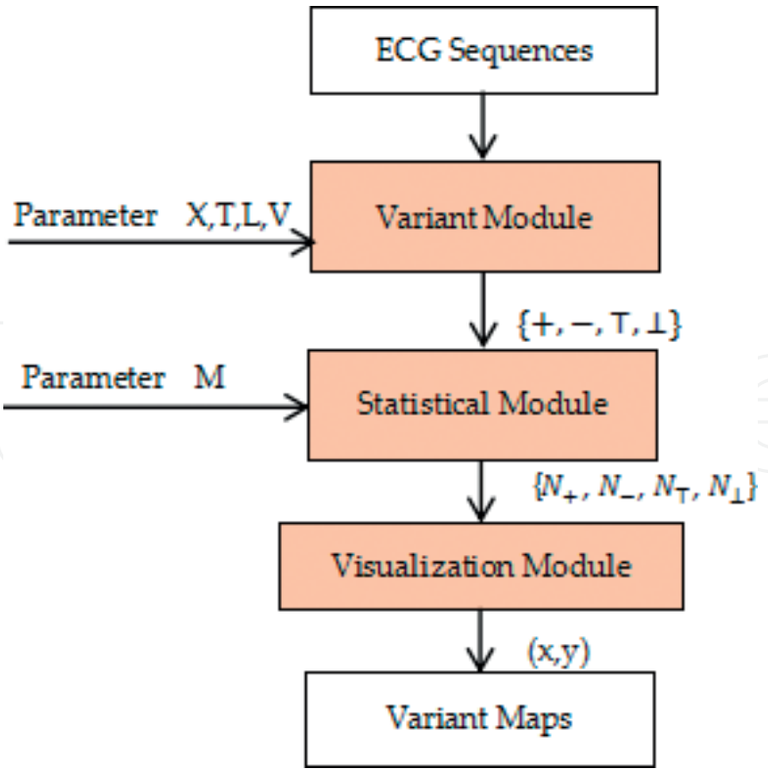

Figure 3.
Structure diagram of ECG data processing.

$$\mathrm{L} = \frac{A_i + A_{i+1}}{2} \tag{3}$$

$$\mathrm{V} = \frac{\sum_{i=1}^{N-1} \frac{(A_i + A_{i+1})}{2}}{N} \tag{4}$$

Considering that the difference value can reflect the increase or decrease of adjacent ECG data, the difference value of the overall ECG data can reflect the fluctuation of the sequence; the mean value can reflect the level of adjacent ECG data, so the mean value of the overall ECG data can reflect the overall level of the sequence. In the process of data transformation, the variant module selects the difference, global difference, mean, and global mean as the measurement parameters. Using the parameters defined in Eqs. (1)–(4), the corresponding X, T, L, V parameter values can be calculated for the input n-long ECG signal sequence as the parameter support of the variant module. According to the mapping principle of Eq. (5), the original ECG sequence was mapped to {+, -, ⊤, ⊥} sequence by setting parameters.

$$\begin{cases} if \;\; X > T \;\; and \;\; X > 0: \;\; B_i = + \\ if \;\; X > T \;\; and \;\; X \le 0: \;\; B_i = - \\ if \;\; X \le T \;\; and \;\; L > V: \;\; B_i = \top \\ if \;\; X \le T \;\; and \;\; L \le V: \;\; B_i = \perp \end{cases} \tag{5}$$

2.7.2 Measurement statistics module

As shown in **Figure 3**, for n-1 long variant logic symbol sequence, set the segment length parameter M, the number of groups is S, and then $S = (n-1)/M$. According to the grouping situation, the number of "+" ,"-" ,"⊤" and "⊥" in each group is recorded

as "N_+", "N_-", "$N_\top$" and "$N_\perp$", "N_+" represents the number of statistics of the variant logic symbol "+" in this group. After statistical process, the whole output group is generated $S\{N_+, N_-, N_\top, N_\perp\}$. For each set of statistical results, including $\{N_+, N_-, N_\top, N_\perp\}$ meet $0 \leq N_+, N_-, N_\top, N_\perp \leq M$, $N_+ + N_- + N_\top + N_\perp = M$, $n-1$ long variant logical symbol sequence is converted into S group statistical array $\{N_+, N_-, N_\top, N_\perp\}$.

2.7.3 Visualization module

The visualization module determines the selection of coordinates (X, Y) and generates a variant graph. According to the results obtained from the measurement statistics module and the definition of variant visualization, this chapter selects overall two-dimensional maps, two-dimensional combination maps, and three-dimensional combination maps to display the visualization results. The overall two-dimensional maps define normal and abnormal ECG signals as $4 * 4 = 16$ of 256 combinations, respectively. The two-dimensional combination maps is to form the scatter diagram of normal and abnormal ECG signals by the same mapping method, and it is easier to observe the differences between them on the same maps. Three-dimensional combination maps are a combination method added on the basis of two-dimensional combination maps. In three-dimensional space, the characteristics between normal ECG signal and abnormal ECG signal are more abundant.

3. Data sets

The ECG data is provided by the people's hospital of Wuxi Xishan. The CB series ECG review analyzer is used to measure blood pressure of ECG data. Through the system of the patient's ECG information is stored in 18 data files, one of .dat files is stored in the patient's ECG data, by reviewing the ECG blood pressure of CB series data of ECG analysis system is read as shown in **Figure 4**.

As shown in **Figure 4**, the patient's ECG was collected with three-lead, and the heart rate data of CH1 lead was recorded at a sampling point of 1.5 s on average. The ECG signal was imported into the database for variant measurement experiment. This set of ECG data includes 105 patients. By analyzing the diagnosis results of each patient, this data set can be divided into two categories: normal and abnormal. Abnormal ECG data includes four types of symptoms: atrial premature beat, 64 cases; ventricular/atrial premature beats and T changes, 9 cases; premature ventricular/atrial beats and complete right bundle branch conduction block, 4 cases; atrial fibrillation and ST-T changes, 4 cases; and normal, 24 cases. In this chapter, atrial premature beat and normal ECG data were selected for variant measurement.

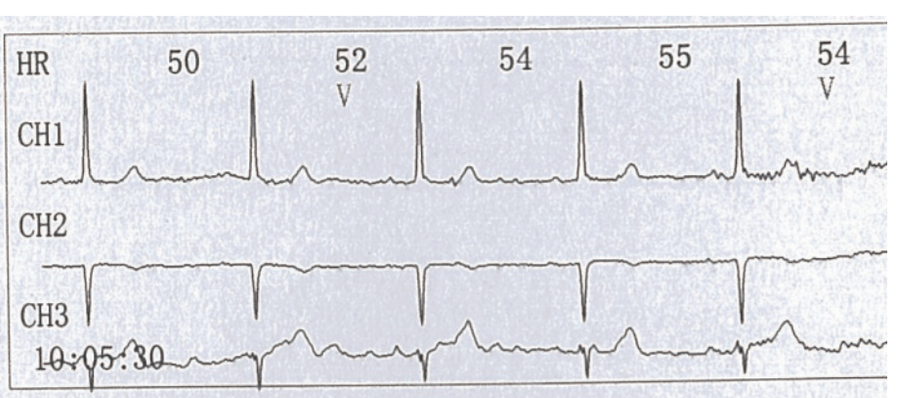

Figure 4.
ECG data diagram of Xishan People's Hospital.

4. Experimental results

4.1 Two-dimensional overall maps

As shown in **Figure 5**, the red diagram on the left is a variant map of normal ECG signals; the blue on the right is a variant map of atrial premature ECG signals,

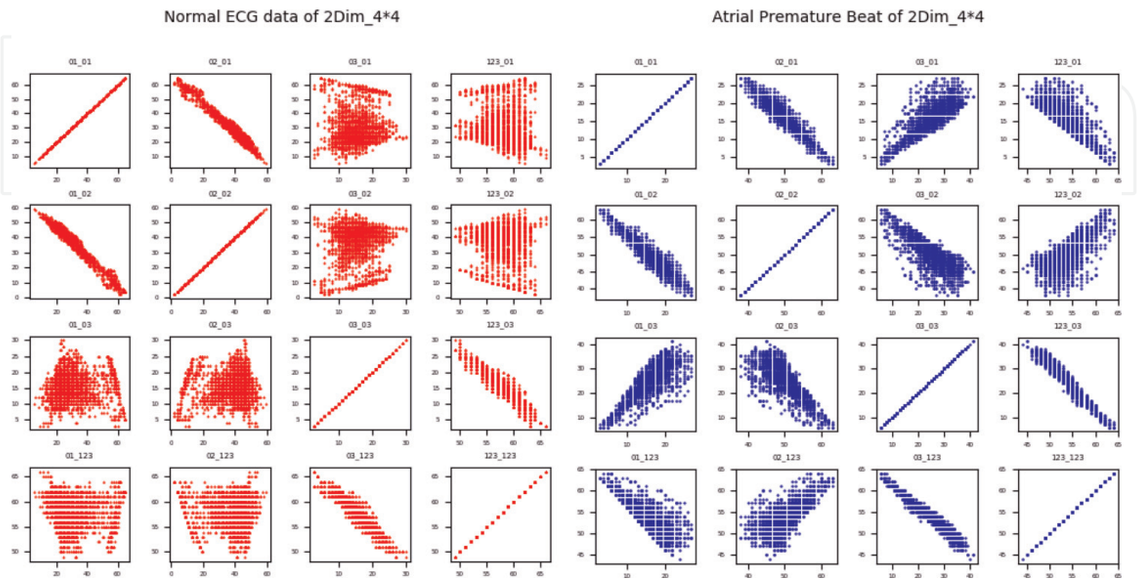

Figure 5.
Overall two-dimensional maps of normal ECG data and atrial premature beat.

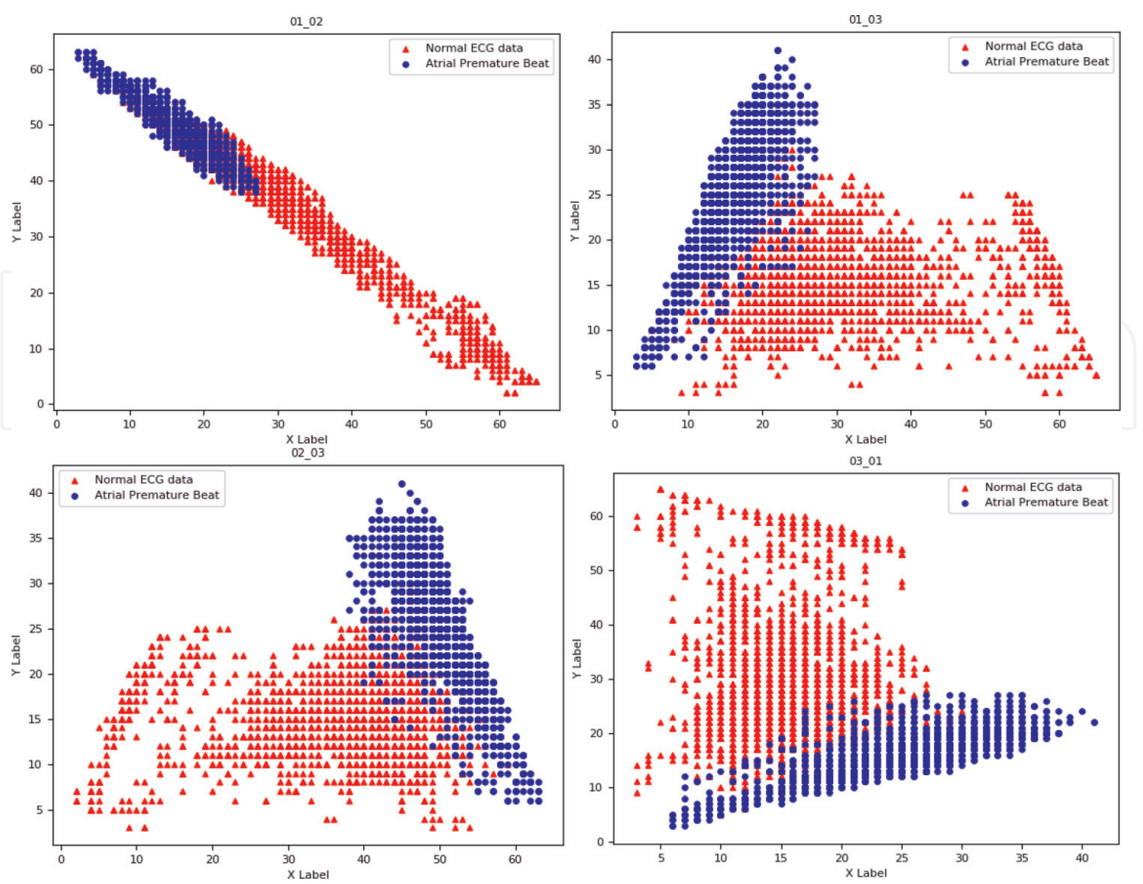

Figure 6.
Two-dimensional combination maps of normal ECG data and atrial premature beat.

with the same mapping of $X = \{M_5, M_6, M_7, M_{14}\}$, $Y = \{M_5, M_6, M_7, M_{14}\}$ formed when the $4 * 4 = 16$ insets. At the top of each small map is the mapping mode corresponding to that diagram.

4.2 Two-dimensional combination maps

As shown in **Figure 6**, the two-dimensional combination maps put the results of the variant of the normal ECG signal and the atrial premature beat ECG signal in one picture, and the four combinations in **Figure 6** are (M_5, M_7),(M_5, M_6),(M_6, M_5), and (M_7, M_6),; the values of X, Y are all limited to the sum of the two subsets.

As shown in **Figure 7**, the two-dimensional combination maps also put the results of the variant of the normal ECG signal and the atrial premature beat ECG signal in a single graph. The 12 combinations in **Figure 7** are (M_5, M_{14}), (M_6, M_{14}), (M_7, M_{14}), (M_8, M_{11}), (M_8, M_{12}), and (M_8, M_{13}), (M_9, M_{11}), (M_9, M_{12}), (M_9, M_{13}) (M_{10}, M_{11}), (M_{10}, M_{12}), (M_{10}, M_{13}), the value of X is limited to the sum of two subsets, and the value of Y is limited to the sum of the three subsets.

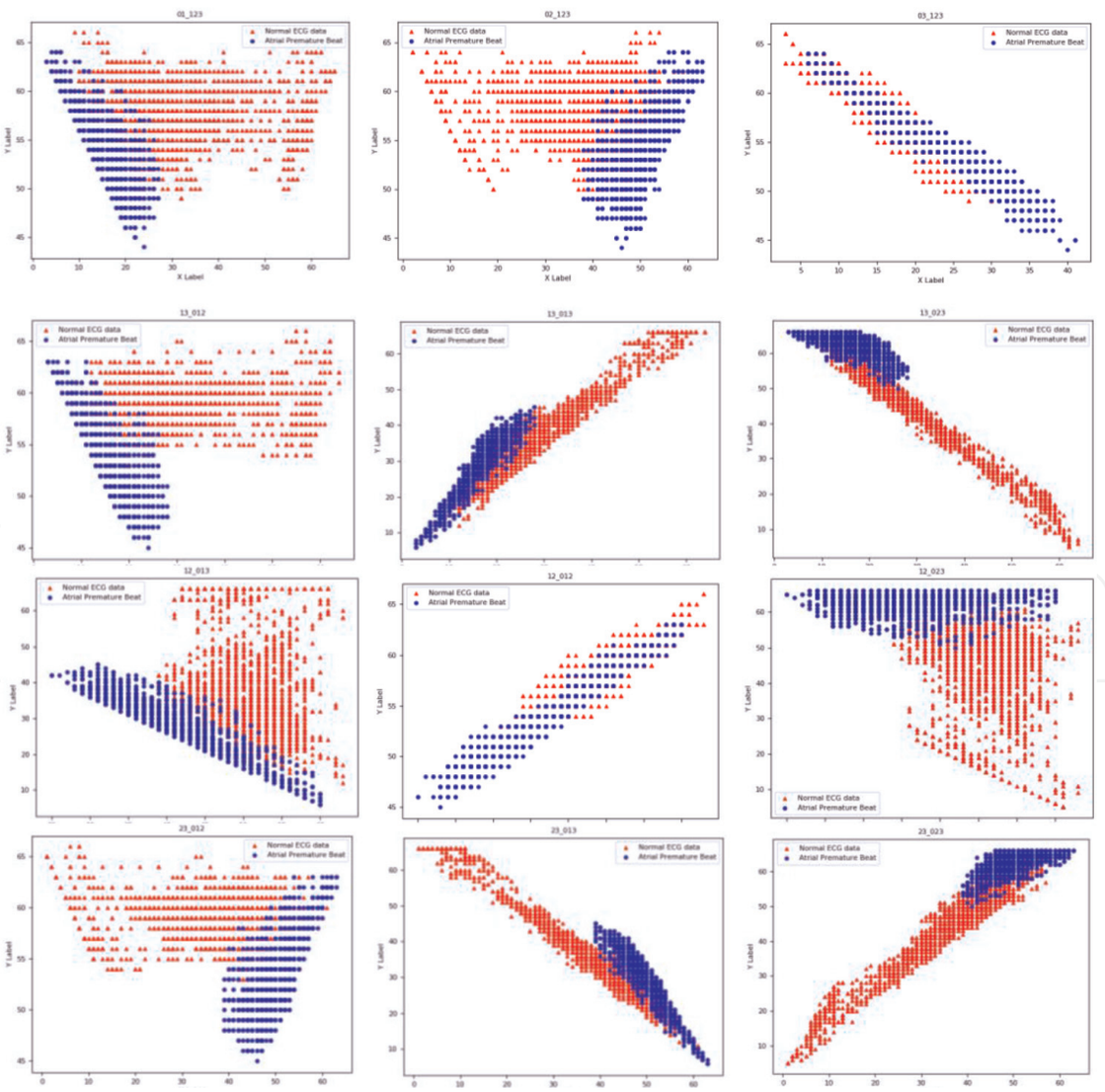

Figure 7.
Two-dimensional combination maps of normal ECG data and atrial premature beat.

4.3 Three-dimensional combination maps

As shown in **Figures 8–10**, the three-dimensional combination maps are a combination of the normal ECG signal and the atrial premature beat ECG signal in the three-dimensional space. The mode of the (X, Y, Z) combination in **Figure 8** is (M_5, M_8, M_{11}), the combination of (X, Y, Z) in **Figure 9** is (M_6, M_9, M_{12}), and the combination of (X, Y, Z) in **Figure 10** is (M_7, M_{10}, M_{13}),; the values of X and Y are both defined as the sum of the two subsets, and the values of Z are all limited to the sum of the three subsets.

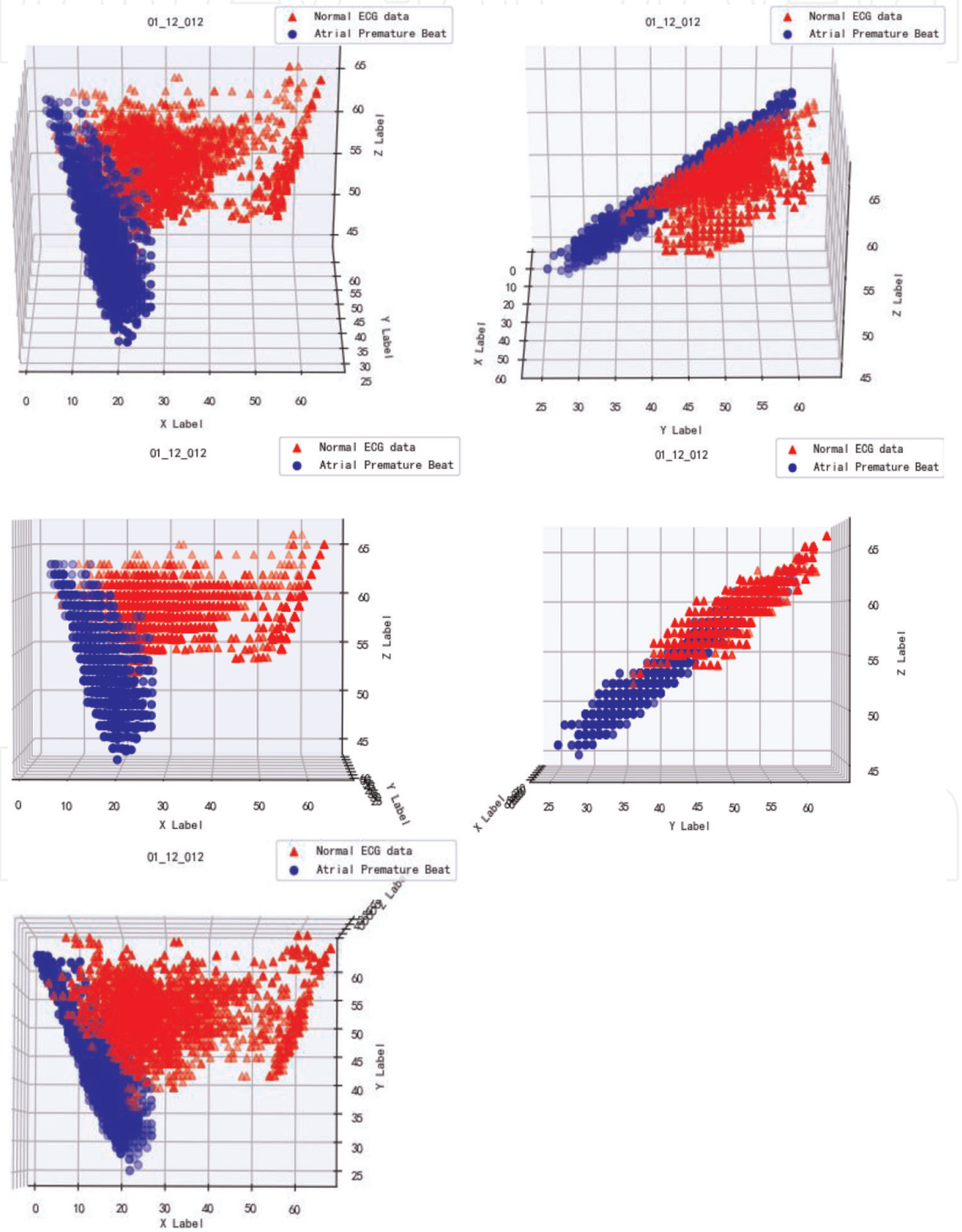

Figure 8.
Three-dimensional combination maps of normal ECG data and atrial premature beat.

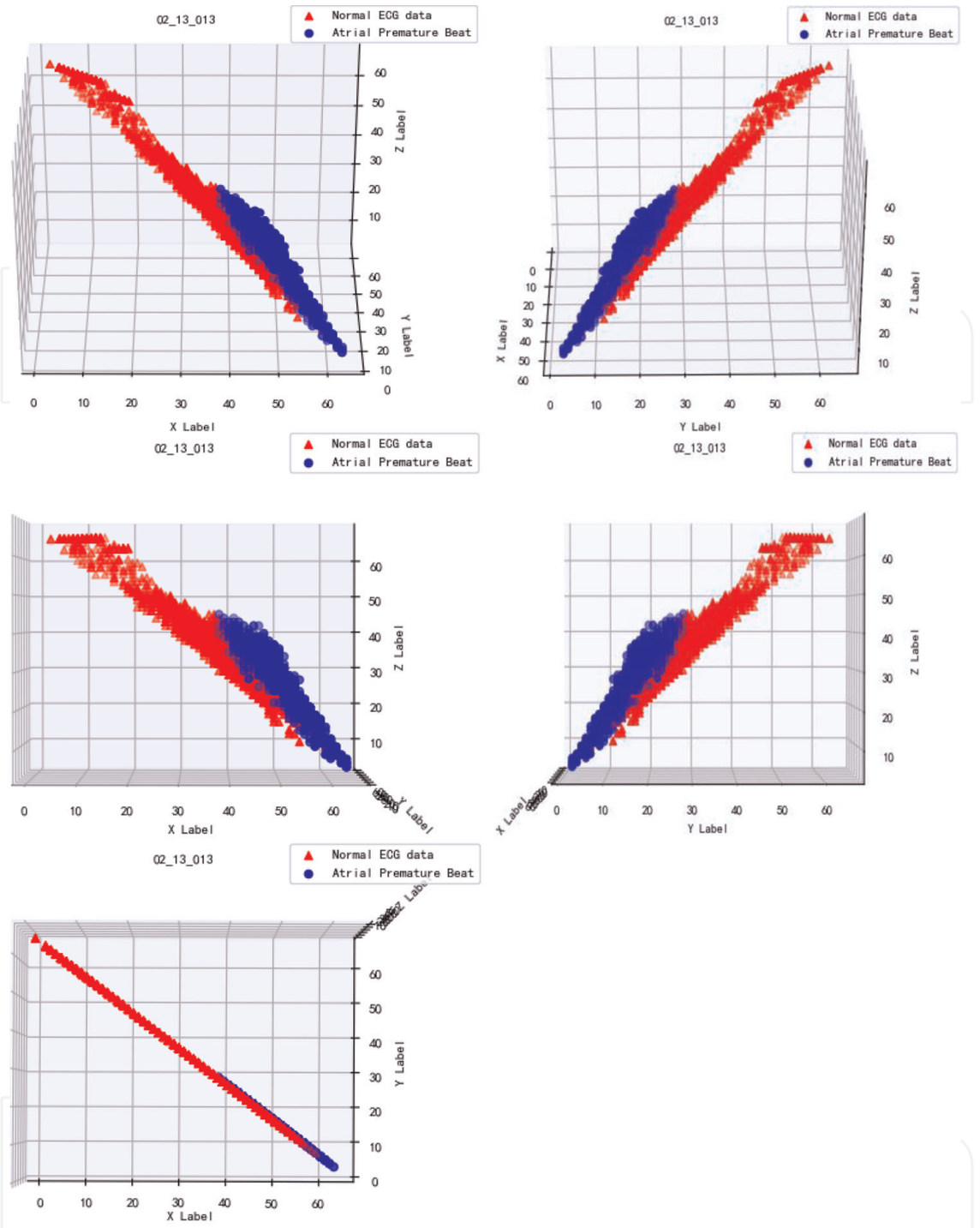

Figure 9.
Three-dimensional combination maps of normal ECG data and atrial premature beat.

5. Results analysis

Through the display of two-dimensional integral maps, two-dimensional combination maps, and three-dimensional combination maps, we can observe that:

The two-dimensional integral maps are to show the macro difference between the normal ECG signal and the atrial premature beat ECG signal through the variant experiment. From the two-dimensional whole figure, there are significant differences in the distribution shape and range between normal and abnormal ECG signals. The variant maps of the normal ECG signal show that the scattered points are disperse, even spreading the entire canvas, and the shape of the atrial premature

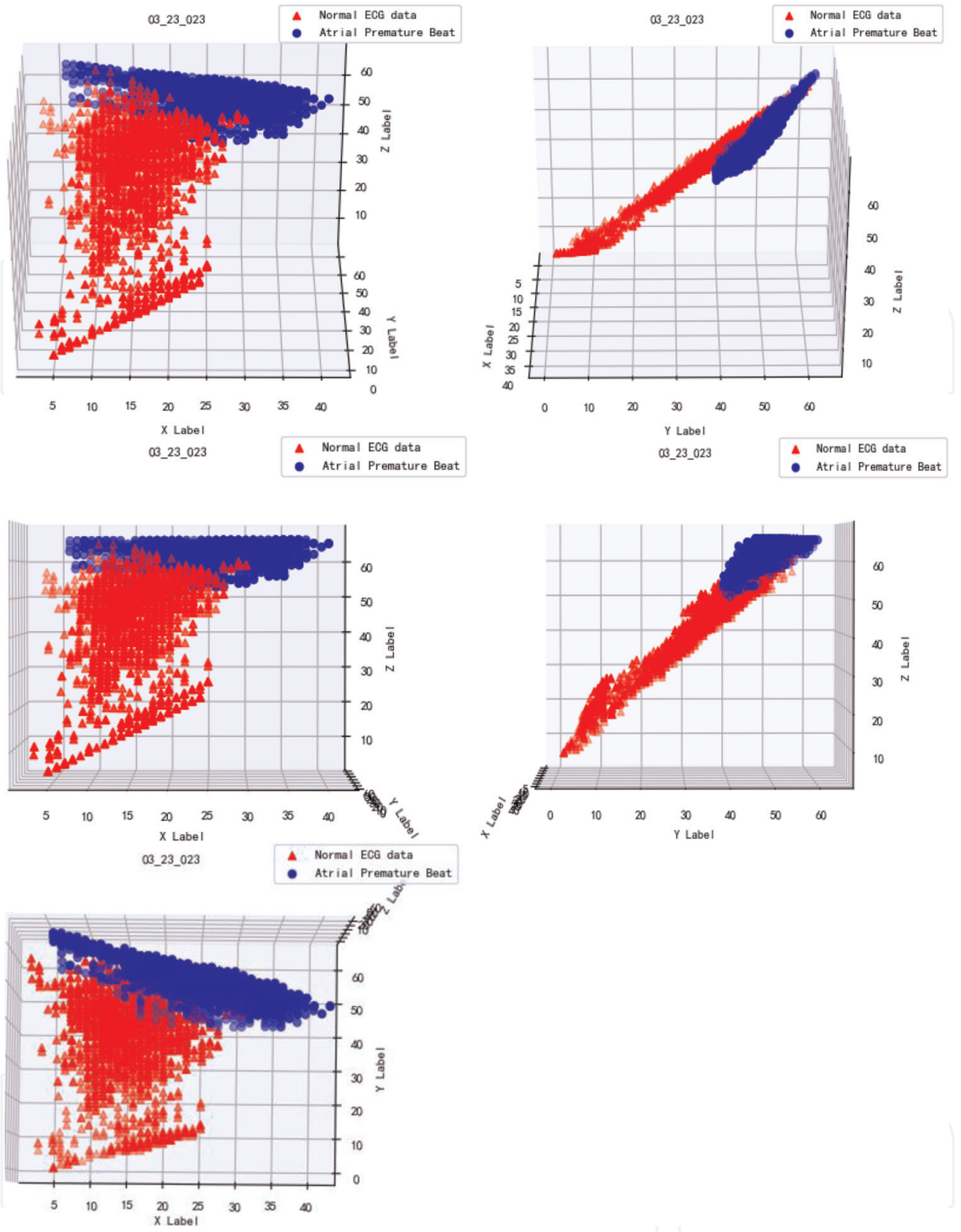

Figure 10.
Three-dimensional combination maps of normal ECG data and atrial premature beat.

beat ECG signal appears as an irregular cone. As the mapping mode changes, the shape of the variant maps also change, but the normal and abnormal ECG signals always exhibit different variant characteristics.

The two-dimensional combination map puts the variant maps of the two types of ECG signals on one canvas, and the difference between the normal and abnormal variant obtained by the same mapping method is more clear on one canvas. The mapping method selected in this chapter is more comprehensive, so the obtained variant map results are also universal.

The three-dimensional combination map is based on the two-dimensional combination maps subjoining the Z-axis to form a spatial distribution display of the

variant maps. The (X, Y, Z) combination of the three-dimensional combination map selects (M_5, M_8, M_{11}), (M_6, M_9, M_{12}), and (M_7, M_{10}, M_{13}), and combines the two subsets and three subsets. The combination of the two is well integrated and is a more comprehensive illustration of the variant of normal and abnormal ECG signals. In the graphic display, five kinds of views are selected for each mapping method, which are (X, Y, Z), (Y, X, Z), (X, Z), (Y, Z), and (X, Y) as the screenshot of the main view. Through the results, we can see that there are also large differences in the three-dimensional spatial distribution of normal ECG signals and atrial premature beat ECG signals.

6. Summary and outlook

In this chapter, the variant measurement model is used to perform the variant experiment on the acquired batch ECG data. Finally, the experimental results of the variant measurement are displayed through three visualization methods. It is found through experiments that the variant measurement model can be well applied to the classification of normal ECG signals and atrial premature beat ECG signals.

In the future, we hope to get more abundant ECG data and can cooperate with the hospital to implement the application of the variant measurement model in the classification of ECG signals, so that it can assist the traditional ECG application in the clinical field.

Acknowledgements

Thanks to the Xishan People's Hospital of Wuxi City of Jiangsu Province for ECG datasets, to First People's Hospital of Yunnan Province for calibrator of ECG data, and to the Key Project of Electric Information and Next Generation IT Technology of Yunnan (2018ZI002), National Science Foundation of China NSFC (61362014), and the Overseas Higher Level Scholar Project of Yunnan for financial supports of the project.

Author details

Lihua Leng[1], Jeffery Zheng[2*] and Jing Zhang[3]

1 Technology and Product Management Department, Agricultural Bank of China, Yunnan Branch, Kunming, China

2 School of Software, Yunnan University, Kunming, China

3 Department of Cadre Health, Yunnan First People's Hospital, Kunming, China

*Address all correspondence to: conjugatelogic@yahoo.com

References

[1] Thompson SC, Ting SA. Avoidance denial versus optimistic denial in reaction to the threat of future cardiovascular disease. Health Education & Behavior the Official Publication of the Society for Public Health Education. 2012;**39**(5):620

[2] Zheng J, Zheng C. Variant measures and visualized statistical distributions. Acta Photonica Sinica. 2011;**40**(9): 1397-1404

[3] Mitchell LB. Atrial Premature Beats. The ECG. Springer. 2004:239-335

[4] Wallmann D, Tüller D, Wustmann K, et al. Frequent atrial premature beats predict paroxysmal atrial fibrillation in stroke patients: An opportunity for a new diagnostic strategy. Stroke. 2007; **38**(8):2292-2294

[5] Zheng J, Zheng C. A framework to express variant and invariant functional spaces for binary logic. Frontiers of Electrical and Electronic Engineering in China. 2010;**5**(2):163-172

[6] Zheng J, Zheng C, Kunii TL. A Framework of Variant Logic Construction for Cellular Automata, Cellular Automata—Innovative Modelling for Science and Engineering. Rijeka, Croatia: InTech Press; 2011

[7] Zheng J, Luo J, Zhou W. Pseudo DNA sequence generation of non-coding distributions using variant maps on cellular automata. Applied Mathematics. 2014;**5**(1):153-174

[8] Zheng J. Novel Pseudo Random Number Generation Using Varian Logic Framework. Australian Security Congress. 2011:100-104

[9] Heim DM, Heim O, Zeng PA, Zheng J. Successful creation of regular patterns in variant maps from bat echolocation calls. Biological Systems: Open Access. 2016;**5**:166. DOI: 10.4172/2329-6577. 1000166

[10] Leng L, Zheng J. Mapping ECG signal sequences on variant maps. In: 2017 IEEE Trustcom/BigDataSE/ICESS; 2017. pp. 881-884. DOI: 10.1109/ Trustcom/BigDataSE/ICESS.2017.326

[11] Leng L, Zheng J. Visualization research of ECG sequence in sinus arrhythmia. Computer Science. 2016;**43** (s2):183-185 (in Chinese)

[12] Zheng J. Variant Construction from Theoretical Foundation to Applications. Springer-Nature. 2019. DOI: 10.1007/ 978-981-13-2282-2